7 An Approach to Performing Aerosol Measurements

PAUL A. BARON and WILLIAM A. HEITBRINK

Centers for Disease Control and Prevention*, National Institute for Occupational Safety and Health, Cincinnati, OH

INTRODUCTION

Today's scientists and engineers making aerosol measurements have available a diversity of aerosol monitors ranging from sample collection on a filter for later analysis to complex direct-reading instruments that detect the airborne particles in real time and display size distribution and chemical data. Instruments used for aerosol measurement frequently provide only an indirect measure of the desired information.[1] For instance, commonly used optical particle counters measure an "optical size" that must then be converted to a physical or aerodynamic size using assumptions about particle properties. Most instruments also only operate over a limited particle size range, and often two or more instruments with different detection principles are used to cover a wider size range. Therefore, the aerosol practitioner must be able to assess the meaning and usefulness of data likely to be obtained with various instruments when selecting one or more for a specific purpose. Use of the simplest or most complex device may introduce errors in measurement and interpretation. While the data from the more complex sizing instruments may make errors evident and indicate the need for corrections, errors also occur in the less-sophisticated filter or inertial collectors. Lack of recognition of these errors may affect the interpretation of aerosol measurements. Approaching the aerosol measurement process with an appropriate plan will reduce the likelihood of major errors in the results.

QUALITY ASSURANCE: PLANNING A MEASUREMENT

In aerosol measurement, the difficulties of selecting an instrument often sidetrack the issue of applying quality assurance principles to obtain accurate and meaningful data. Many scientists prefer to address problems in a more investigative fashion. However, many of the principles of quality assurance can be integrated into this approach with relatively little effort and with large benefits in accuracy and efficiency. Quality assurance principles have been developed over many years, and programs applying these principles are present in most

*Mention of company or product name does not constitute endorsement by the Centers for Disease Control and Prevention.

Aerosol Measurement: Principles, Techniques, and Applications, Second Edition, Edited by Paul A. Baron and Klaus Willeke.
ISBN 0-471-35636-0

analytical laboratories around the world. It has been recognized that reliable data are much more likely to be produced by laboratories under such conditions. The following series of steps is one approach to quality assurance and was developed by the U.S. Environmental Protection Agency (EPA, 1994). It should be recognized that the process is usually a cyclic one: after one pass through the following steps, the steps are repeated until an optimal measurement approach has been achieved.

State the problem: Writing down the problem with a complete indication of the various parameters needed, along with the resources available, will help clarify the likely solutions to the measurement process. For instance, the emission of aerosol from a manufacturing process is contaminating a second process. The transfer of contaminant must be controlled.

Identify the decision: Specifying the decision with appropriate levels of confidence will indicate the complexity of measurement needed to carry out the measurement. In the example above, we need to determine the lowest cost-control measure that prevents the occurrence of cross contamination.

Identify the inputs to the decision: What data are needed to reach the decision? Do we need to measure the size distribution of aerosol and transmission paths throughout the plant or just identify when aerosol concentration at the second process has been sufficiently reduced?

Define the study boundaries: It is often easy to design elaborate experiments to measure parameters that do not contribute significantly to the final decision. Measuring the size distribution of the contaminating aerosol may help understand the process of transfer, but may not necessarily contribute to the final result.

Develop a decision rule: This is a statistical statement of the confidence expected in the data such that the decision can be made.

Specify limits on decision error: This presents a statistical "target" for the measurements to be made.

Optimize design: This is the step that uses experience gained in the initial data collection to refine and improve the previous steps. For example, initial experiments may indicate contamination from unexpected sources or pathways, or the results may be at the limit of the measurement instrument, suggesting that alternate measurement techniques may be better.

MEASUREMENT ACCURACY

If "measurement processes are to serve both the practical needs of humankind and excellence in the pursuit of new scientific knowledge, they must be endowed with an adequate level of accuracy. . . . Control, and acceptable bounds for imprecision and bias, are clearly prerequisites; but scientific conventions (communication) and scientific and technological means for approaching 'the truth' must also be considered" (Currie, 1992). Although nomenclature provides the basis for communication of accuracy of the measurements, the basis for developing the accuracy limits on measurements comes from experiments, assumptions, and scientific knowledge.

Although a formal quality assurance process may seem like overkill for each aerosol measurement process, understanding the principles of a good quality assurance program can highlight or alert the scientist to pitfalls in a proposed experimental approach. There are texts available on quality assurance principles. An example of detailed requirements of such a program applied to environmental measurements are available from the EPA web site (www.epa.gov/region10/www/offices/oea/qaindex.htm).

The discussion below presents problems that can occur when making aerosol measurements. These problems are presented to instill some caution into the practitioner when performing aerosol measurements. There are many measurement techniques presented in following chapters, and it may appear difficult to choose among these techniques. However, based on the desired aerosol property, time resolution, instrument size, resource constraints, and the accuracy required, the choices are often narrowed to one or two approaches. The chapters in Part II, Techniques, start out with techniques that involve collection of particles with subsequent analysis of the collected material (i.e., integral concentration measurements). Then, real-time instruments that collect particles and analyze them are discussed, followed by direct-reading instruments that present information about individual particles (usually size distribution). The final chapters in Part II present information that applies to all measurement techniques: sampling, data presentation, and instrument calibration.

SIZE RANGE

One of the first factors to consider in the selection of instrumentation for aerosol measurement is the size range of the aerosol. Chapter 6 presented size ranges encountered in several environments. Additional examples are given in this chapter and in Part III, Applications. At the small particle end of the spectrum, aerosol particles can form and grow from (photo)chemical reactions, condensational nucleation and growth, and coagulation or agglomeration. At the upper end of the spectrum particles are likely to be formed from mechanical action, such as abrasion and crushing, while droplets can be formed by spraying and bubbling. The typical dividing line between the small and large aerosol particles is about 1 μm, with the former types of aerosols rarely growing significantly above several micrometers and the latter aerosols rarely extending below about 0.5 μm. The type of system generating the aerosol can often give a clue to the particle size range likely to be produced. For example, hot processes such as smelting are likely to produce submicrometer fume particles, mechanical processes such as drilling tend to produce large particle dusts, while some processes such as welding and grinding may produce multimodal distributions covering a wide size range. A number of aerosol measurement instruments are mentioned here with only a very cursory description of their detection mechanism and capabilities. Further details are provided in the indicated chapters covering specific instruments.

The past 30 years of aerosol measurement research has been quite active, with explorations of different detection, classification, and analysis techniques. Some of these techniques have become successful commercial instruments, while others have languished for a variety of reasons. These include inaccuracy, insufficient sensitivity, lack of appropriate application, difficulty of use, high cost, or better competing techniques. There is a continual effort to build aerosol instruments that measure one or more useful aerosol properties over a wider size range. In most cases, the aerosol measurement process is a compromise, with the selection of the available instrumentation that measures an aerosol property closely related to that desired. In general, the smaller the corrections and the fewer the assumptions in conversion factors needed to provide the desired result, the better the information is likely to be. This makes the selection of instrumentation for a given application somewhat of an art.

Although there is not a strict separation between the two, there are two general approaches to aerosol measurement: *collection and analysis* and *direct-reading sensors*. The former is generally less expensive in capital investment, more time consuming, gives integral concentration measures, and allows qualitative and quantitative measurement of the aerosol. The latter approach requires much more expensive instrumentation, usually gives size distribution information, gives nearly instantaneous results, and allows many measurements to

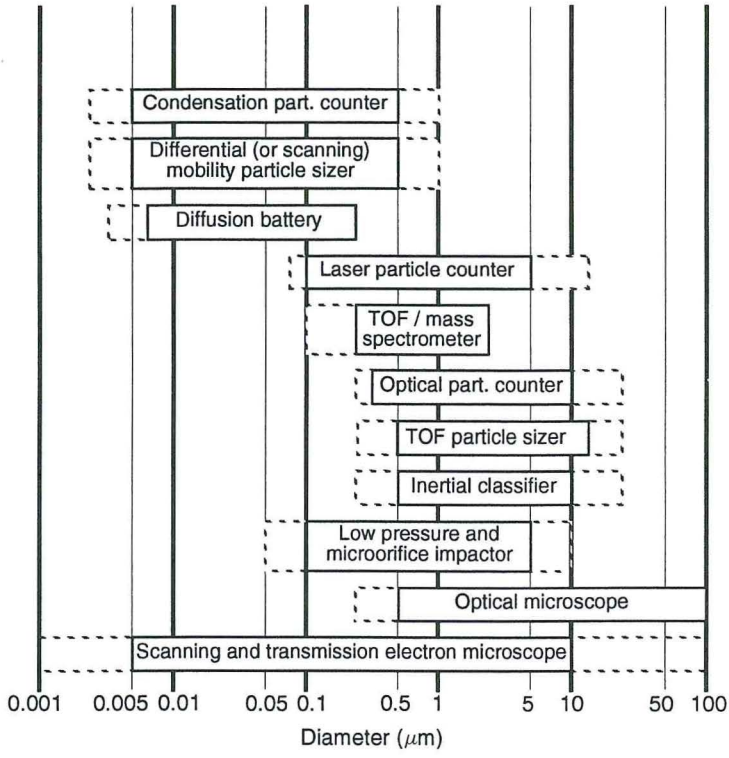

Fig. 7–1. Measurement size range of some principal aerosol sizing and analytical instruments. TOF, Time of flight. (Adapted from Pui, 1996.)

be made over time. An overview of the size range of several types of commonly used classes of instruments is presented in Figure 7–1, and a flow chart indicating the application of some of these and other instruments is presented in Figure 7–2.

COLLECTION AND ANALYSIS MEASUREMENTS

The most common collection technique involves the use of filters for collecting particles from the air. Most modern sampling filters are virtually 100% efficient for all particle sizes (see Chapter 9). The filter is placed in a holder that depends largely on the application. If the sampling device is intended to be a stand-alone device that collects particles from an environment, the enclosure and inlet of the device must be appropriately designed to give accurate, or at least known, sampling efficiency. The aspiration (or entry) efficiency and internal losses in various devices are discussed in Chapter 8. Sampling devices are frequently designed for specific applications, and some of these are discussed in Part III.

In addition to simply collecting all particles entering the sampling device, some instruments are designed to classify particles into two or more size fractions. Inertial separation devices, such as cyclones and impactors, are most commonly used for this purpose. A cyclone causes air to move in a swirling motion from which larger particles are deposited onto a

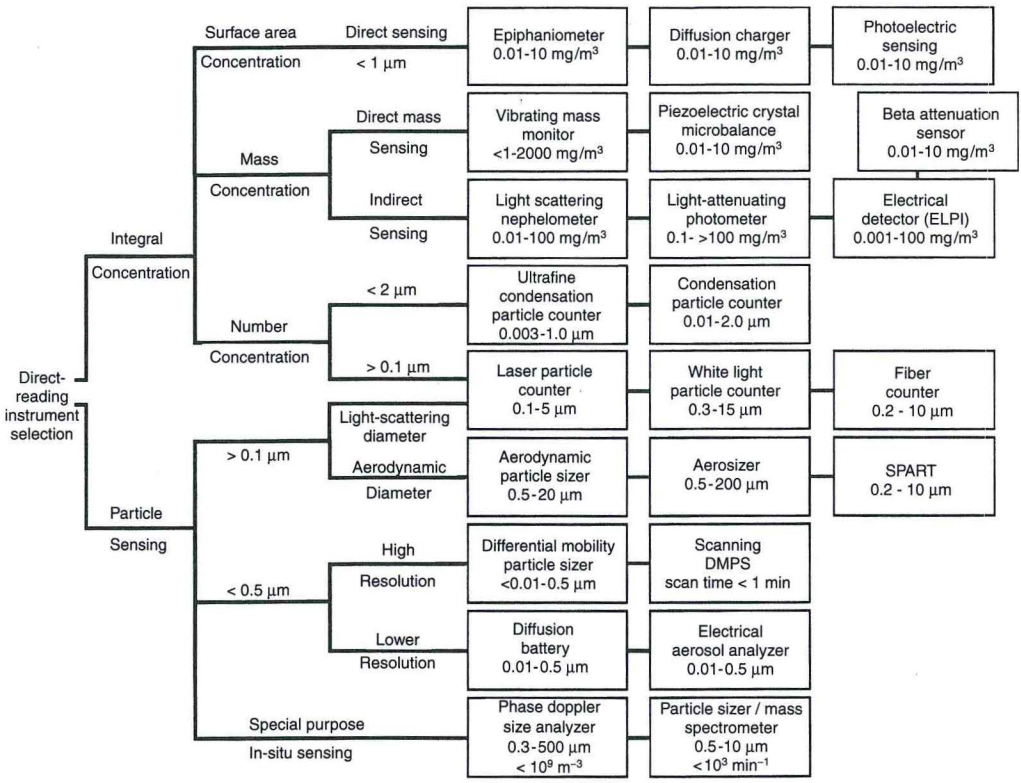

Fig. 7–2. Flow chart for selecting a direct-reading instrument for analyzing aerosol particles. (Adapted from Pui, 1996.)

surface by centrifugal action, while impactors cause a more abrupt change in airflow direction, also causing larger particles to be deposited onto a surface or substrate. For instance, a cyclone or impactor is often placed before the filter (as a "pre-classifier") to simulate the removal of particles by the upper respiratory system so that the material collected on the filter simulates particles reaching the gas exchange region of the lungs (see Chapters 25, 26, 27, and 29).

Particles collected on the filter can be analyzed in many different ways. The sample on the entire filter can be subjected to gravimetric, chemical, biological, or radioactive emission analysis (see Chapters 11, 24, and 34), or individual particles on the filter can be subjected to various forms of microscopy, spectroscopy, or shape analysis (see Chapters 12 and 23).

Classification or size distribution measurement of aerosols can be achieved by placing several classifiers in series as a "cascade." Typically, each stage collects larger particles than the subsequent stages. These devices have various names: cascade impactors, cascade centripeters, cascade cyclones, or diffusion batteries, depending on the separation mechanism. The first three are inertial separators, while the latter separates by a diffusional mechanism. Inertial separators remove larger particles from the air stream first, depositing them onto a clean or greased surface or a filter. The amounts collected on each stage of the cascade can then be analyzed to allow calculation of the size distribution (see Chapters 6 and 22).

Generally, the size classification is performed in a series of steps in which the size cuts decrease by a factor of about 1.5 to 2 from one stage to the next smaller one.

For classification of particles in the submicrometer range, diffusion batteries can be used. These devices consist of several screens or collimated hole structures that allow particles to diffuse to the surface (see Chapter 19). The material collected on the screens or structures can be analyzed (e.g., for radioactivity or chemical composition). The size resolution of these devices is generally much poorer than that of impactors (see Chapters 19 and 22) or electrical classifiers (see Chapter 18), but they are relatively inexpensive.

DIRECT-READING MEASUREMENT OF AEROSOLS

Direct-Reading Measurement of Collected Particles

A wide range of physical and chemical principles have been applied to the detection and analysis of collected particles. Some of these approaches have resulted in direct-reading instruments. For various reasons, few of these devices have survived as commercial instruments. Several of these techniques are described in Chapter 14. Radioactive aerosol monitors are described in Chapters 34 and 35. Perhaps the most common aerosol particle property measured is the mass.

The most direct approach to mass measurement is the deposition of particles onto a vibrating surface and measurement of the change in resonant frequency. Two distinct types of instrument use this approach. The first uses a piezoelectric crystal as the collection surface. This provides high sensitivity and accurate mass measurement, but only for relatively small and sticky particles and only in very limited regions of the crystal. Large particles (several micrometers) may not couple well to the vibrating surface and may be poorly detected. The crystal has vibrational nodes on its surface, and the particles must be precisely deposited on the appropriate nodes to achieve consistent response. For additional description, see Chapter 14 and Williams et al. (1993).

Another vibrational sensor is the Tapered Element Oscillating Microbalance (***R&P***).* The collection substrate, either a filter or an impaction surface, is placed at the end of a tapered vibrating tube. The amount of mass collected on the substrate is related to the decrease in the resonant vibrational frequency of the tube. This approach appears to have fewer artifacts, although variations in temperature, humidity, pressure, and external vibrations can sometimes affect the accuracy of the measurement (see Chapters 14 and 26).

Another approach to mass measurement is the use of β-radiation scattering from collected material. The sample detector places the sample between a β-radiation source and a detector. The radiation is scattered by the electron cloud around the atoms of the sample, attenuating the radiation reaching the detector. The amount of attenuation is approximately proportional to the mass of material, although materials with low atomic number (e.g., hydrogen) have reduced scattering efficiency and are thus underdetected. Hydrocarbon compounds thus require a different calibration than most other materials.

A more recent development is the use of electrical charge to measure the concentration of particles on the individual stages of a cascade impactor (Electrical Low Pressure Impactor [ELPI], ***TSI***; see Chapter 14). Particles are charged as they enter the instrument, and the amount of charge transferred to each impactor stage by the impacted particles is measured with an electrometer. Each stage has a calibration constant that is a function of the charging efficiency for particles collected on that stage and is determined by weighing the portion of a representative test aerosol collected there.

*See Appendix I for full manufacturer addresses referenced by the italicized three-letter codes.

Light scattering from a larger volume than in optical partical counters is used to measure an integral scattering function that averages the signal over particle type and size distribution. This technique provides a rapid readout device that can sometimes be calibrated to give particle mass if the aerosol does not change significantly with time. These devices are called *nephelometers* or *photometers* and some are used as hand-held aerosol indicators in workplace or indoor air, while other more sensitive devices are used for measuring visibility and level of light scattering in the outdoor environment (see Chapters 15 and 16).

Direct-Reading Surface Area Measurements

Several approaches have been developed to measure aerosol particle surface area. One approach is to expose the aerosol to an ion field and measure the net charge accumulated by the particles. In the ELPI, size segregation of particles is accomplished after charging to measure size-dependent surface area. Number and mass distributions are calculated from these data. Another instrument uses charging in a similar fashion, but without size segregation to give total surface area. The epiphaniometer exposes the aerosol to a radioactive gas that decays to radioactive metal atoms, which diffuse to the aerosol particles' surface. The gas is removed before detection, and the resulting radiation detected is indicative of the total particle surface area. A third approach to surface area measurement uses short wavelength light to produce electron emission from the surface of the aerosol particles. The charge detected is a function of surface area and may also be specific for certain chemical species. See Chapter 14 for a discussion of these techniques.

Direct-Reading Measurements of Individual Airborne Particles

Direct reading instruments in this class generally separate or classify particles according to size, but require a particle sensor that responds quickly and efficiently to each particle. The most widely used sensor is the *optical particle counter* (OPC). In an OPC, particles pass through a sensing zone that is illuminated by either a broadband (white light) or a monochromatic (laser or light-emitting diode) source. If the instrument uses a laser, it may be called *a laser particle counter* (LPC). The light scattered by each particle is detected over a range of angles and converted to an electronic pulse that is a complex, but generally increasing function of particle size. Light scattering provides a relatively inexpensive, nondestructive, high-speed technique for particle detection. An OPC can be used for obtaining information about individual particles or for determining total particle concentration, for example in clean rooms (see Chapters 15, 16, and 33). With the appropriate optics, OPCs can be designed so that the sensing volume is external to the instrument, thus allowing the measurement of particles in extreme environments, such as outside of aircraft in the atmosphere (see Chapter 30) or in high-temperature stacks or reactors (see Chapter 31).

Optical particle counters are used as stand-alone instruments to detect and size particles. However, the light scattered by each particle has a complex dependence on the light source, the range of detection angles, the particle size, particle shape, and the particle refractive index. It is usually difficult to predict or compensate for the latter two factors in real-world situations, and thus the sizing capability of OPCs is usually only approximate.

In the small particle size range, particle detection by light scattering loses sensitivity, with a lower limit of about 0.1 μm under optimum conditions. To detect particles smaller than 1 μm, the OPC is often aided by condensational growth of small particles in the condensation particle counter (CPC), also called a condensation nucleus counter (CNC). The CPC exposes particles to a supersaturated vapor that condenses onto particles. All the particles grow to approximately the same size (on the order of a micrometer) and can then be detected by light scattering. The CPC can detect particles down to several nanometers and, under certain conditions, even size particles in the 1 to 3 nm range (see Chapter 19).

Direct-Reading Particle Size Distribution Instruments

Small Particle Size Range. There are several forms of the electrical mobility classifier that allow size separation of submicrometer particles. These devices operate by providing a known fraction of the particles with one electrical charge each and subjecting the particles to an electric field. Particles that achieve a selected velocity in the electric field (i.e., a selected electrical mobility) pass through the classifier and can be detected, usually with a CPC. Several of these devices have been developed and commercialized, each optimized for a specific size range or application (see Chapter 18). These devices can provide high-resolution size information in the range of a few nanometers to about 0.5 μm within several minutes. Larger particles are not sized accurately because they are likely to retain multiple charges.

Diffusion batteries can also be used as direct-reading instruments by detecting the particles passing through the diffusive collecting elements with a CPC. However, because of the inherently lower resolution of the size separation elements, diffusion batteries have significantly lower resolution than the electrical mobility classifiers. The size distribution must be deconvoluted from the diffusion battery's raw penetration data, and the deconvoluted spectra are subject to significant errors (see Chapters 19 and 22). Although these devices are less costly than the electrical mobility instruments, they have largely lost favor as direct reading instruments and are used primarily as integral sampling devices, as noted above.

Large Particle Size Range. The most common instruments for particle sizing are the OPC and the LPC, which can operate over a relatively wide range of concentration and size. The LPC generally produces a higher intensity beam at the sensing volume, resulting in higher sensitivity to small particles. Solid-state lasers are available with shorter wavelength that can also be used to detect smaller particles. These instruments provide rapid readout and moderate size resolution. They are subject to complex sizing errors as a function of particle parameters, as noted above, but for many applications provide a lower cost solution. Some of the errors in sizing can be reduced by appropriate calibration with the aerosol being measured (see Chapters 15 and 21).

The time-of-flight particle sizers sample the aerosol through a nozzle, accelerating the particles so that their velocity is a function of particle aerodynamic diameter. The velocity of the particles is measured by the time of flight of the particles through the sensing zone. The high acceleration through the nozzle produces non-Stokesian effects in the sizing process, and corrections usually have to be applied to obtain true aerodynamic diameter. However, the corrections, especially for known density and gas viscosity, are predicted from theory and can be accurately applied. These spectrometers can provide high-resolution spectra in less than 1 minute and give reasonably accurate results. Because of the relative complexity of these instruments, the sizing and concentration errors, although usually not great, sometimes can be subtle and difficult to correct (see Chapter 17).

One of the ultimate goals of aerosol measurement is to provide a complete analysis (e.g., size and chemical analysis) of individual particles in real time. A new type of instrument approaches this goal, although in a very expensive and rather bulky, yet movable, package (see Chapter 13). The time-of-flight sizing principle has been coupled with a laser ablation system and a mass spectrometer to produce particle size–dependent chemical information about an aerosol. There are significant limits to the size range and concentration that this instrument can measure, but it can provide information virtually unattainable by other means.

AEROSOL MEASUREMENT ERRORS

Figure 7–3 summarizes some major sources of biases that may occur in an aerosol measurement. The original unsampled aerosol may range in particle size from about 0.001 to about 100 μm. Various portions of this range may be nondetectable with a given measurement tech-

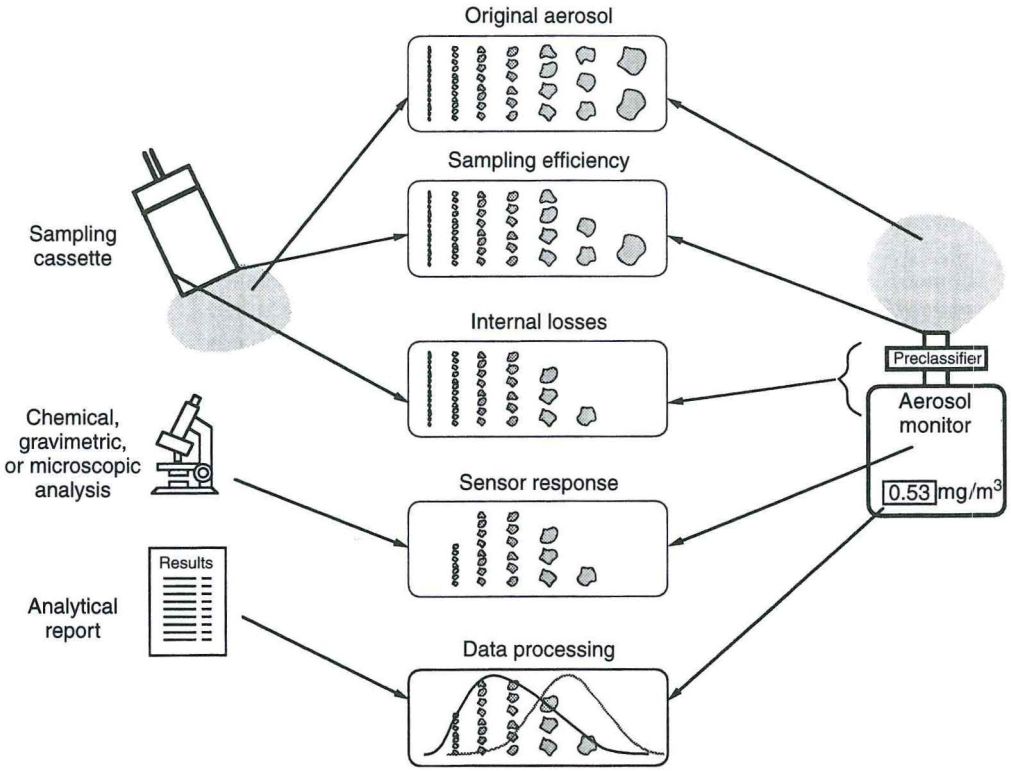

Fig. 7–3. Schematic representation of some important biases in aerosol monitoring. (Adapted from Willeke and Baron, 1990.)

nique. Particles smaller than about 20% of the wavelength of visible light (0.4 to 0.7 μm) are generally not detectable by optical means. Depending on the purpose of sampling and the type of aerosol present, different portions of this 0.001 to 100 μm size range may be of interest. For instance, the health scientist's concern has often focused on the 0.5 to 10 μm size range because the aerosol particle mass within this size range is likely to deposit in the biologically sensitive regions of the respiratory system. Measurement of such aerosols will be used as an example in some of the following discussion, parts of which have been adapted from Willeke and Baron (1990).

As the aerosol enters the sampling inlet of the aerosol measuring device, the ratio of ambient air velocity to sampling velocity, the air turbulence, as well as the size, shape, and orientation of the inlet, may affect the sampling efficiency of the inlet (Vincent, 1989; Okazaki et al., 1987a,b). Generally, the larger particles enter less efficiently, as illustrated in Figure 7–3, because of properties producing inertial losses and particle settling. Various particle size pre-classifiers, such as cyclones or elutriators, take advantage of these properties to impose size discrimination on sampled particles. Some of these devices are tailored to allow only a certain fraction of particles to pass through for detection. Aerosol particles reaching one specific region of health concern (i.e., the alveolar or gas exchange region of the lung) is defined as respirable dust. A cyclone is generally used to measure respirable dust as defined by the American Conference of Governmental Industrial Hygienists (ACGIH) definition of respirable dust, while a horizontal elutriator is used for the British Medical Research Council (BMRC) definition (ACGIH, 1984).

The section connecting the inlet to the collection device (e.g., filter) or sensor (e.g., detection region of photometer) is usually considered separately from the inlet or the point at which the aerosol enters the measurement device. For instance, in asbestos sampling a length of tubing equal in diameter to the filter collection area called a *cowl* (Baron, 1994) connects the sampling inlet to the collecting filter. In a direct-reading monitor, the aerosol is generally transported from the inlet to the sensor via a tube or channel. Particle losses may occur in these channels due to electrostatic attraction, impaction, or gravitational settling and further reduce the aerosol concentration, generally in the upper size range as illustrated in Figure 7–3. For devices with small inlets sampling submicrometer particles, diffusion may also contribute significantly to the losses. Thus, it is important to make this connection region out of conductive material to reduce electrostatically induced losses and, furthermore, to minimize the length of this region to reduce losses due to other forces.

When a filter sample is analyzed under a microscope, particles smaller than the wavelength of the illuminating light may not be detected efficiently. For an electron microscope, that wavelength is much smaller than for an optical microscope. Thus, the microscope and the human eye discriminate against detection of smaller particles. Other types of analysis also may have size-dependent biases introduced during sample preparation or analysis. The sensor of a direct-reading aerosol monitor has a lower threshold below which the smaller particles remain undetected, as illustrated in Figure 7–3. The upper size limit of detection is generally less of a problem for the sensor. However, most sensors do not respond equally to all particles of varying size and shape. This further modifies the measurement process. Sometimes, as with the electron microscope, the process of viewing particles can change the shape, state, or chemistry of the particle. Often these effects cannot be changed, but must be recognized during the analysis of the data.

A further bias can occur with instruments such as optical particle sizing instruments that depend on having only one particle at a time in the detector view volume. If more than one "coincide" in the view volume, the sensor only registers one particle, possibly of a larger size (Willeke and Liu, 1976). More complex instruments may produce more complex coincidence effects, modifying the observed size distributions in unusual ways (Heitbrink et al., 1990). These coincidence errors usually can be reduced by lowering the particle concentration (e.g., by inserting a dilutor before the sensor).

Data processing involves collection, storage, and analysis of the data. If too few particles have been sampled, the displayed particle size distribution may not reflect the true size distribution because of statistical considerations. If the particles are counted as a function of particle size under the optical microscope or in situ by an optical sensor, the volume or mass can be calculated for each particle, thus shifting the "weighting" from a "count" distribution to a "volume" or "mass" distribution. Various assumptions in this weighting procedure can bias the resulting distribution. The assumption of particle sphericity is usually an approximation, except for droplets. Because the particle volume depends on the cube of the particle size, a few large particles outweigh many small particles. Thus, presentation of the particle size by "count" for most naturally occurring aerosol size distributions focuses on a smaller size range than the size distribution weighted by "volume" or by "mass." The number of particles in the relevant size range, therefore, statistically limits the accuracy of the recorded aerosol concentration, indicating that a sufficient number of particles must be collected in the size range of interest.

The type of display, whether it is a histogram or a cumulative plot, emphasizes different aspects of the size distribution. Finally, the method of size calibration plays an important role in the accuracy of the results. For example, if a photometer or optical single particle counter is calibrated with particles that scatter but do not absorb light, an absorbing aerosol, such as coal dust, will be registered as having a smaller than actual particle size.

In the following sections, the aerosol size distributions used to demonstrate some of the above points were calculated using the Aerosol Calculator program (see Chapter 2). This

type of program allowed the rapid calculation of lognormal size distributions (using Eq. 8–4) that can exist in sampled atmospheres, as well as how these distributions might be affected by biases and variability that occur with these measurements. The program used Eq. 7–1 for calculation of the number fraction (Δf) of particles in a size interval ranging from $\ln d$ to $\ln d + \Delta \ln d$ for a diameter d_i:

$$\Delta f = \frac{1}{\sqrt{2\pi}\ln\sigma_g}\exp\left[-\frac{(\ln CMD - \ln d_i)^2}{2(\ln\sigma_g)^2}\right]\Delta \ln d_p, \tag{7–1}$$

where CMD is the count median diameter of the lognormal distribution for which σ_g is the geometric standard deviation. Published sampling and measurement efficiency data were used to modify these lognormal distributions. Note that the number concentrations calculated were based on equal size increments on a log scale (i.e., $\Delta \log d_p$ = constant) so that the ordinate in each graph is $\Delta N/\Delta \log d_p$, where N is in the units of number of particles/m^3. Some curves were scaled to give a desired peak concentration.

The variability present in actual aerosol measurements of finite numbers of particles was simulated in some cases. Because aerosol particles arrive at a detector or sampler at random times, the count variability was described by a simulated Poisson distribution within each size increment. This variability was introduced by adding to each size increment a random number that was normally distributed (on the square root scale) about zero and had a variance equal to the particle count in that size increment.

In the following sections, some of the sources of bias and variability in measurement and interpretation are examined in more detail for some specific measurement situations. Note that this approach to calculating size distributions provides a convenient means of data analysis, both for planning experiments and for understanding published data.

Sampling and Transport

The measured size-dependent sampling efficiencies for the open and closed face 37 mm cassettes (Buchan et al., 1986), both widely used in industrial hygiene sampling with filters, have been multiplied by the corresponding values of an example lognormal size distribution with a median diameter d_{50} = 5.0 μm and a geometric standard deviation σ_g = 2.0 (Fig. 7–4). These samplers are used for a variety of dust measurements, and a smaller diameter version of the cassette is used for asbestos exposure measurement (Baron, 1994). Two sampling efficiency curves are calculated for an open and a closed face sampler hanging down with the inlet perpendicular to a horizontally moving wind stream of 100 cm/s; the third curve was calculated from measurements with the sampler on a mannequin facing the wind under the same wind conditions. The mannequin-mounted sampler curves were nearly identical for closed and open faced cassettes so a single average curve has been drawn for this case. It is apparent that the air flow conditions near the sampler inlet can significantly affect the collection efficiency of the sampler. The bluff mannequin body reduced the effect of wind speed on the sampler inlets. As pointed out in Chapter 6, the inlet efficiency is optimum when the air flow velocity and direction in the sampler and surrounding air are exactly or nearly matched. In Figure 7–4, there is a size-dependent reduction in particle concentration relative to the true concentration that varies with sampler placement.

Electrostatic attraction to the cassette inlet and its walls reduces the amount collected on the filter, especially if the cassette is constructed of nonconducting material (Baron and Deye, 1990). The loss increases with the number of electrical charges on the aerosol particles and on the sampler and decreases with increasing sampling rate. The number of charges on airborne particles depends on the process producing the particles, the air humidity or the amount of water on the particle surface during release, and the length of time the particles have been airborne (see Chapter 18). Direct-reading aerosol monitors may have similar sam-

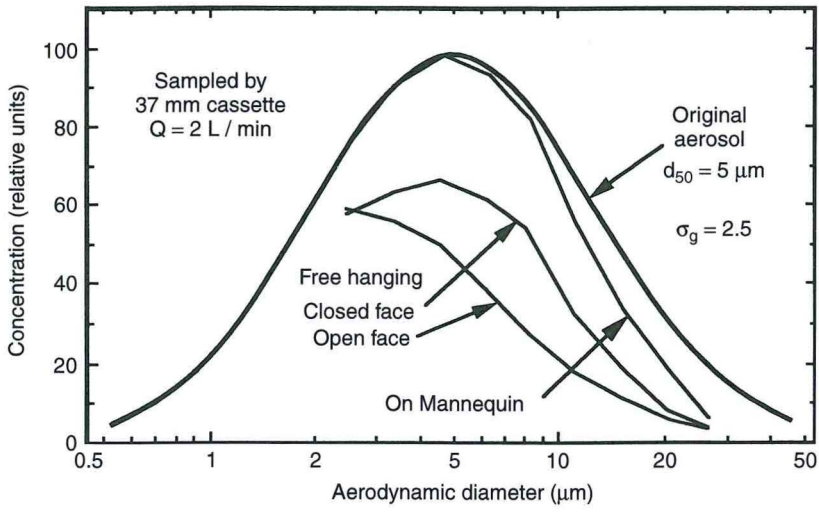

Fig. 7–4. Sampling and transport biases in several cassette configurations. Sampling efficiency data were taken from Buchan et al. (1986) and smoothed. Cassettes hung on a bluff body (a mannequin) appear to have smaller biases than free-hanging ones (Adapted from Willeke and Baron, 1990).

pling and transport losses, depending on the design of the inlet and the section leading to the sensor (Liu et al., 1985).

Sensor Sensitivity and Coincidence Effects

When the particles collected on a filter are analyzed by optical microscopy, many of the small particles are not detected by the microscopist, with none being counted below a certain size, say, 0.3 μm. The smaller particles of the original aerosol size distribution are thus not counted. If, in addition to inlet losses, the filter does not collect particles with 100% efficiency, the sample available for analysis may be further modified.

The combined effect of sensor response and inlet losses are illustrated for the Aerodynamic Particle Sizer (APS, ***TSI***), a time-of-flight aerosol spectrometer that uses light scattering to detect particles. To illustrate the effect of a sensor's size-dependent sensitivity, a lognormal size distribution with mass median aerodynamic diameter $d_{50} = 1\,\mu m$ and $\sigma_g = 2.5$ is calculated to simulate the measured aerosol (Fig. 7–5). Based on measured efficiency curves of Blackford et al. (1988), there is a modification of the "measured" size distribution at the low end due to a lack of detector response and at the high end due to a loss of particles at the instrument inlet. Note that neither of these losses changes rapidly with particle size and that the resulting distribution appears nearly lognormal. These modifications of the shape of the distribution may result in incorrect interpretation of the shape of the original aerosol distribution.

If the sensor is an optical device receiving a light-scattering signal each time a particle passes through the view volume, particle coincidence (i.e., simultaneous presence of two or more particles in the view volume) may result in the detection of a single larger particle, producing a slight shift to larger sizes and reducing the observed particle number over the entire size range. The importance of coincidence effects increases with particle number concentration.

In a time-of-flight device, such as the APS or the Aerosizer (***TSI***), the time of flight of a particle accelerated between two path-intersecting laser beams is a measure of its aerody-

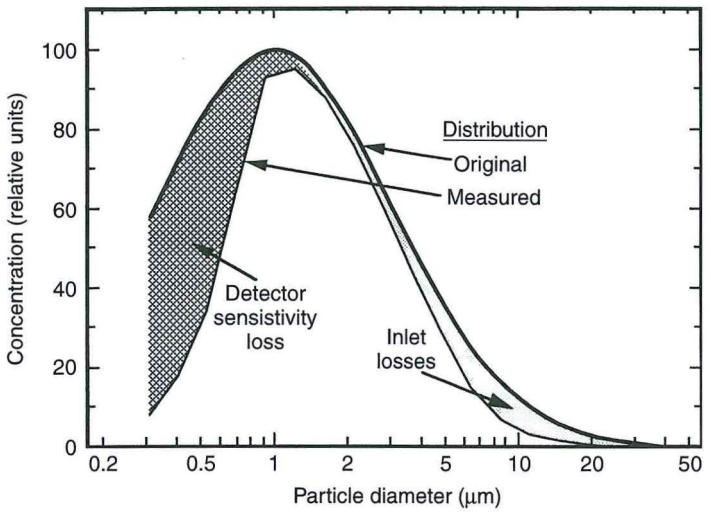

Fig. 7–5. Sensor bias data for the Aerodynamic Particle Sizer (APS3300) taken from Blackford et al. (1988). (Adapted from Willeke and Baron, 1990.)

namic liameter. These instruments can have coincidence losses like other optical particle counting instruments. In addition to a loss of particle counts, these instruments may produce a background of artifactual or phantom counts (due to more than one particle in the sensor at a time) at all particle sizes that may overshadow the fewer correctly detected particles at the tails of the distribution (Heitbrink et al., 1991). These phantom counts can be especially important if the distribution is converted to a mass distribution (a few large, phantom particles may outweigh the rest of the distribution) or if the data are used for comparison measurements (Wake, 1989), for example, the ratio of concentrations upstream and downstream of a cyclone.

Aerosol sensors of different types may be used to measure the same parameter, such as particle aerodynamic diameter (d_a). This can provide some estimate of the biases present in the measurements. However, when the readings from different instruments result in widely disparate readings, a detailed understanding of the detection and sampling processes can be used to estimate the "best" answer. A comparison of several measurement techniques used on a grinding wheel aerosol to measure aerodynamic diameter is shown in Figure 7–6 (O'Brien et al., 1986). Filter samples were analyzed by scanning electron microscope (SEM), and real-time measurements were made with two OPCs (Model CI-108, ***CLI***; Model ASAS-X, ***PMS***), a quartz crystal microbalance cascade impactor (Model PC-2 [instrument type discontinued], California Measurements, Berkeley), and an APS. The results from instruments not measuring aerodynamic diameter d_a (defined as the diameter of a unit density particle having the same gravitational settling speed as the particle in question) were converted to d_a. Such a conversion is generally made in health effect studies because gravitational settling and inertial impaction of particles in the human respiratory tract in the size range of about 0.5 μm and higher are directly dependent on aerodynamic particle diameter (Hinds, 1999).

One can make a best estimate of the aerosol d_a distribution based on knowledge of the size-dependent sensitivities of the instruments and the correction factors applied to each instrument's data. With the SEM and OPCs, relatively large correction factors based on assumed average particle shape, density, and refractive index may culminate in

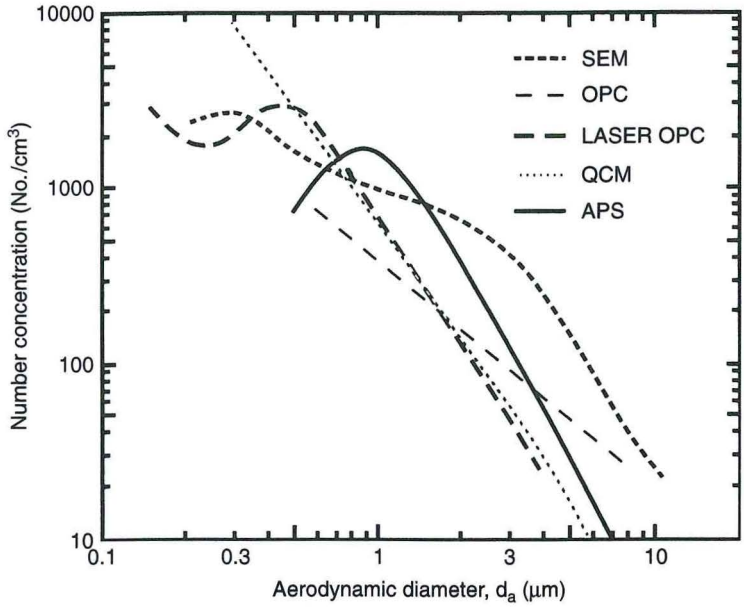

Fig. 7–6. Measurement of grinding wheel dust using six different measurement techniques, including a scanning electron micrograph (SEM), two optical particle counters (OPC), a quartz crystal microbalance cascade impactor (QCM), and an APS3300 (APS). (Adapted from O'Brien et al., 1986.)

relatively unsatisfactory results. The grinding aerosol was a difficult aerosol for such a comparison because of the presence of a number of materials with widely disparate properties.

Particle Statistics

Assuming that particles in an aerosol have been detected by a direct reading instrument, the distribution of particles can be simulated using the Aerosol Calculator spreadsheet indicated above. For a lognormal aerosol size distribution with a number median diameter of 2.5 μm and a geometric standard deviation of 2.0, the smooth number distribution curve calculated in Figure 7–7a results from a relatively large total count of 1 million particles distributed in 19 size increments over the size range 0.2 to 45 μm. Such a high particle count is realistic for dynamic sensors whose data acquisition systems permit multichannel analysis, but might overload a filter that must be analyzed by microscopy.

The surface area and the volume for each particle size may now be calculated. The surface area and volume of each size, multiplied by the number of particles in the respective size ranges, results in the distributions also shown in Figure 7–7a. The peak of each distribution is normalized to 100 relative units for illustration purposes. Inclusion of the particle density would allow conversion of the volume to a mass distribution. The representation of the aerosol size distribution by any of these weightings (count, surface, or volume) results in a smooth curve because a large number of particles was used.

When the total count is reduced to 1000 (Fig. 7–7b), the number distribution curve is still recognizable as approximately lognormal, although the additional variability due to a smaller count in each size increment is apparent. Example 7–1 indicates how to perform

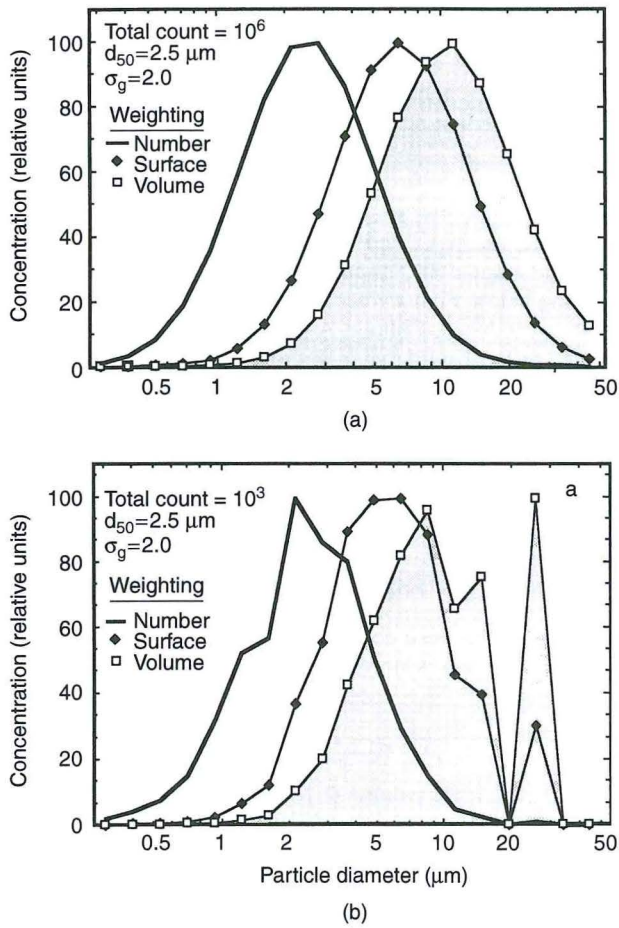

Fig. 7–7. Variability in volume, or mass, measurements. Surface area and volume distributions calculated from high (**a**) and low (**b**) particle count are given, and the curves are normalized to the same height. The volume variability at low count is due to statistical fluctuations, especially in the tail of the number distribution. (Adapted from Willeke and Baron, 1990.)

this calculation using the Aerosol Calculator. However, the surface distribution emphasizes the larger particles, of which there are fewer. The variability in particle count for these larger particles is greater. The volume or mass distribution (highlighted by shading) emphasizes even larger particles resulting in a poorly determined curve. Conversion of a count distribution to a volume or mass distribution by counting an insufficient number of particles, may, therefore, result in considerable imprecision. Figure 7–7b illustrates and emphasizes the need for measuring a large number of particles in the particle size range of interest. Several modern real-time aerosol monitors are computer based and offer easy conversion from one weighting to another. Such easy conversion may tempt the user to accept numbers that may have inherent biases and high variability. Note that the variability in mass due to a small number of large particles applies also to gravimetric measurements when small samples are obtained.

EXAMPLE 7–1

Calculate the number, surface and volume values for a lognormal distribution of spherical particles with a count median diameter of 5 μm and σ_g of 2. Simulate the variability as if the entire distribution contains approximately 1000 particles.

Answer: The following equations were developed in the spreadsheet program Excel (Microsoft Corp., Bellevue, WA) and were implemented in the Aerosol Calculator sizedis.xl module (see Chapter 2). The input values and constants are listed in the first four rows in the listing below. First we need to generate the diameters for which the lognormal distribution is produced. Column A has numbers starting at 0.25 with each following row multiplied by a constant factor, in this case 1.32, giving 19 size intervals or bins between 0.25 and 49 μm. The starting size and size interval can be changed to span the range of other size distributions if desired. The second column is the geometric mean of the upper and lower endpoints of each bin and is the size used to represent that bin. Thus, A6 to A7 is the first size interval and the geometric center of that interval is B6 $= \sqrt{A7 \times A6}$. C6 uses Eq. 7–1 to determine the concentration function in that bin or size interval.

$$C6 = ((A7 - A6) / (\$E\$1 * B6 * \$E\$3)) * EXP\left(-\left((LN(B6) - \$E\$2)\text{^}2\right) / \left(2 * (\$E\$3\text{^}2)\right)\right)$$

The "$" indicates that the reference does not change in the following rows, i.e., in C7, C8, etc. The concentration function is normalized to give the appropriate number of total counts, in this case 1000.

$$D6 = C6 * \$E\$4 / \$C\$25$$

C25 is the sum of all the values in column C. Next "noise" is added to the normalized particle density function to simulate the counting process. The following function produces a random number that is part of an approximately normal distribution, centered about zero with a standard deviation σ (Hansen, 1985)

$$\sigma = \sqrt{12n}\left[\left(\frac{\sum_{i=1}^{n} RAND_i}{n}\right) - 0.5\right]$$

where n is usually chosen to be a number 3 and $RAND_i$ is a random number between 0 and 1 that can be generated by the computer. The larger the value of n, the closer the resulting distribution will approximate a normal distribution, especially in the tails of the distribution. The Poisson distribution approaches a normal distribution for large particle counts, so this function provides a reasonable approximation to a Poisson distribution. Poisson statistics require that the variance of the particle counts be equal to the mean count. Thus the standard deviation of the count in each bin is equal to the square root of the value of the density function, i.e., the count in that bin. The function is rounded to integer values as would be produced by a counting instrument.

$$E6 = ROUND(D6 + ((((RAND() + RAND() + RAND() + RAND() + RAND()) / 5) - 0.5) * SQRT(60) * SQRT(D6)), 0)$$

where RAND() is a function that generates a random number between 0 and 1. E6 is the value for the number distribution. The surface and volume distributions are calculated from this distribution assuming spherical particles.

F6 = E6 * PI( ) * B6^3

G6 = E6 * PI( ) * B6^3/6

Finally, if one wishes to normalize the peak value of the distributions to the same value, e.g., 100, as in Figure 7–7, three more columns, H, I, J can be created that contain the normalized number, surface and volume distributions. These have not been included in the table below due to space considerations. H6, I6, and J6 would contain E6·100 / E25, F6·100 / F25, and G6·100 / G25, respectively. E25, F25 and G25 contain the maximum values in their respective columns. Note that the columns E, F and G (as well as H, I and J) will always appear somewhat different than indicated below since the random numbers will produce different results.

Further, sampling or detection efficiencies such as those indicated in Figure 7–4 and 7–5 can be calculated by multiplying the normalized density function (column C) by those efficiencies.

TABLE 7–1. Spreadsheet Size Distribution Calculation from Example 7–1 (Using the Aerosol Calculator Described in Chapter 2)

	A	B	C	D	E	F	G
1	d(50) =	5	SQRT (2*π) =		2.5066		
2	σ(g) =	2	LN (d(50)) =		1.6094		
3			LN (σ(g)) =		0.6931		
4	total	number of	particles =		1000		
5		diameter (μm)	Δf	Number	No. With Random Count	Surface	Volume
6	0.2500	0.2872	3E-05	0.03	0	0	0
7	0.3300	0.3791	0.0002	0.16	1	0.452	0.029
8	0.4356	0.5005	0.0006	0.65	1	0.787	0.066
9	0.5750	0.6606	0.0023	2.25	3	4.113	0.453
10	0.7590	0.8720	0.0067	6.69	4	9.556	1.389
11	1.0019	1.1511	0.0170	16.93	19	79.09	15.17
12	1.3225	1.5194	0.0366	36.50	30	217.6	55.10
13	1.7457	2.0056	0.0673	67.08	71	897.2	299.9
14	2.3043	2.6474	0.1052	104.96	110	2,422	1,069
15	3.0416	3.4946	0.1403	139.88	119	4,565	2,659
16	4.0149	4.6128	0.1592	158.79	154	10,294	7,914
17	5.2997	6.0889	0.1540	153.54	156	18,170	18,439
18	6.9956	8.0374	0.1268	126.45	122	24,759	33,167
19	9.2342	10.609	0.0890	88.71	81	28,643	50,646
20	12.189	14.004	0.0532	53.01	62	38,200	89,161
21	16.090	18.486	0.0271	26.98	19	20,397	62,843
22	21.238	24.401	0.0117	11.70	14	26,188	106,502
23	28.035	32.209	0.0043	4.32	5	16,296	87,482
24	37.006	42.517	0.0014	1.36	0	0	0
25	48.850		1.0027	1,000	156	38,200	106,502

Corrections for Density and Other Physical Properties

Curve A in Figure 7–8, shows a smooth, calculated representation of an aerosol size distribution with a median aerodynamic diameter of 5.0 μm and $\sigma_g = 2.0$. This aerodynamic particle diameter can be converted to physical particle diameter. The conversion is achieved by dividing the aerodynamic particle diameter by the square root of the particle density (see Chapter 3). A shape factor to account for nonspherical shapes also needs to be included in the conversion, but is not discussed here. For coal dust, which has a higher than unity particle density ($\rho_p \approx 1.45\,g/cm^3$), the physical diameter (curve B, Fig. 7–8) is smaller than the aerodynamic diameter. Thus, a particle of a given physical size settles in the same region of the respiratory tract as a physically larger, but less dense particle.

Curve A in Figure 7–8 represents the actual aerodynamic diameter distribution of a coal dust aerosol to be measured using an OPC. Typically, these counters, as well as photometers, are calibrated with spherical, nonabsorbing test aerosols such as dioctyl phthalate (DOP) or polystyrene latex spheres (PSL). For example, DOP has a refractive index $m = 1.49$ (no imaginary or absorptive component). All the light received by these test particles is scattered from the particles. However, if the particles are light absorbing, such as coal dust ($m = 1.54$ to $0.5i$, with 0.5 representing the absorptive component of the refractive index), a particle of a given size scatters less light. Therefore, a coal dust particle scatters much less light and appears much smaller than a similar-sized test particle; the particle size distribution is recorded to be in a smaller size range, as illustrated by curve C in Figure 7–8 (Liu et al., 1974). In addition, the size correction for the absorbing particle, such as coal dust, may be strongly particle size dependent, further distorting the measured size distribution. Although the distortion and shifting of the size distribution for coal dust is an extreme case, the assumptions involved (spherical particles, refractive index, and density values) illustrate some of the pitfalls of using optical sizing data to determine aerodynamic size.

An optical particle counter uses the optical properties of the individual particles for size discrimination. It therefore needs to be calibrated for the aerosol it measures. Other types of aerosol monitors use different physical properties for size discrimination. An electrical size

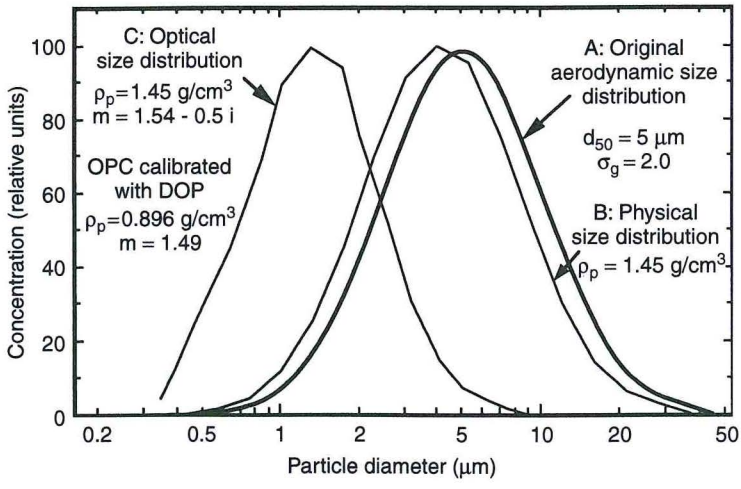

Fig. 7–8. Measurement of coal dust using various physical properties of the particles (density, ρ_p, and refractive index, m). Curve A represents the aerodynamic size distribution of a coal dust sample; curve B represents the physical size distribution of that dust (correcting for density); and curve C represents the measurement of the coal dust by an optical particle counter (OPC) calibrated with monodisperse dioctyl phthalate (DOP) particles (Liu et al., 1974). (Adapted from Willeke and Baron, 1990.)

classifier, for example, uses the electrical mobility of particles for size discrimination of submicrometer aerosols. Because the composition of the aerosol to be measured may be unknown, inadequate calibration may prevent the "size" obtained with one type of aerosol monitor from equaling the "size" obtained with another instrument.

Presentation of Size Distribution Data

There are several ways of presenting measured size distributions, each with advantages and disadvantages (see Chapter 22). Assume that two dusts are present in the air: dust 1 with a median diameter of 1.5 μm and dust 2 with a median diameter of 10 μm, both with a geometric standard deviation of 2.0. Measurement of the aerosol with a direct-reading aerosol size spectrometer is simulated using the Aerosol Calculator to give the bimodal size distribution shown in Figure 7–9A.

If this measurement is replotted on a cumulative plot where the value of the ordinate indicates the number of particles less than the given size, the wavy plot of Figure 7–9B results. Starting with the smaller particles, the curve increases with increasing particle size in an S-shaped manner. At sizes slightly larger than the median size of dust 1 the curve levels off and then increases in slope again as the median size of dust 2 is approached. This type of presentation is common for the results of low-resolution instruments such as a cascade impactor.

If one does not know that there are two dust modes present, one may be tempted to draw a straight line through the cumulative plot, as indicated by the heavy straight line in Figure 7–9B. This is frequently done and justified by attributing the deviation of the data from a straight line to experimental variability. The resulting graphically estimated or "measured" aerosol thus has a geometric median diameter of about 3.4 μm (corresponding to the minimum between the two dusts) and a geometric standard deviation of 3.5, indicating a single dust distribution much broader than each of the modes in the original bimodal distribution. Potentially valuable information is lost in this representation of the data because multiple modes usually indicate different sources of aerosol.

Some statistical tests may also indicate that the cumulative data in Figure 7–9B do not fit a single distribution. For instance, the Kolmogorov-Smirnov test (Gibson, 1971) would indicate whether the measured distribution fits a single mode distribution, and a plot of residuals (the differences between the measured and calculated values) qualitatively indicates whether adjacent measurements in the curve are correlated or whether the data fit the single lognormal distribution model.

Both types of representation have advantages and disadvantages. The differential plot gives a better presentation of the distribution shape: Modes show up directly, and any effect of bias is constrained to a narrow size range and is not propagated throughout the entire size distribution as in the cumulative plot. The cumulative plot provides a better estimate of the median diameter of the aerosol and allows easier presentation of data graphically without using a computer. Frequently, investigation of the data through several display techniques affords a more complete understanding of the physical meaning of the data.

Particle Size Selection

The type of aerosol monitor used depends on the purpose of sampling. The industrial hygienist generally samples from a health perspective. Because the physiological shape of the human respiratory system determines the region in which the particles will deposit, a pre-classifier is frequently mounted ahead of the sensor in order to intentionally limit the particle measurement to particles reaching the physiological region of concern. For example, a cyclone, impactor, or elutriator pre-classifier can separate the aerosol into respirable and nonrespirable fractions.

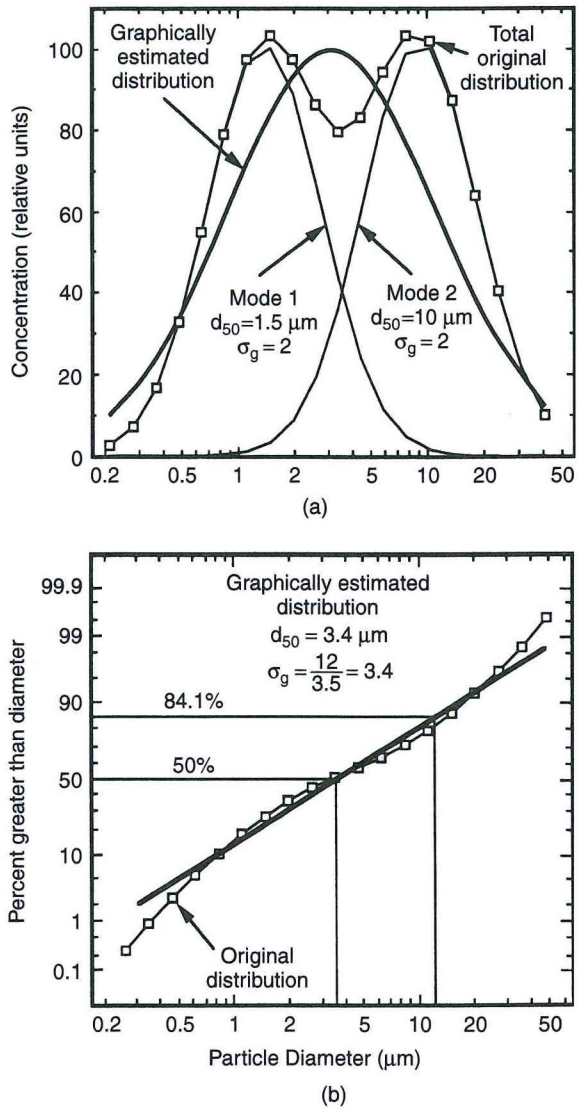

Fig. 7–9. Representations of a bimodal size distribution: histogram (**A**) versus log probability plot (**B**). It is possible to misinterpret the log probability plot of a bimodal distribution as being from a single mode. (Adapted from Willeke and Baron, 1990.)

The respirable mass fraction can also be obtained by sensor discrimination. Size distribution results can be weighted appropriately in each size range to give the respirable dust response (Baron and Willeke, 1986). Aerosol photometers are relatively inexpensive, direct-reading instruments that have a built-in size discrimination sometimes used for respirable dust measurements (Baron, 1994). Such light-scattering devices monitor the scatter of light from an aerosol cloud rather than from single particles. Figure 7–10 illustrates this for a specific photometer, the TM digital μP (***HUN***).

Figure 7–10 shows the calculated instrument response per unit mass concentration as a function of particle size for two kinds of aerosols with the same aerodynamic size distribu-

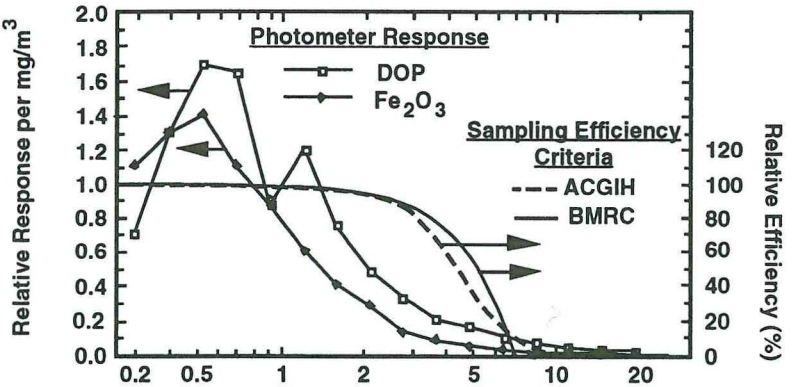

Fig. 7–10. Respirable mass response using a photometer for example size distributions of two materials with $d_p = 5\,\mu m$, $\sigma_g = 2.0$. Detection efficiency is for the TM Digital μP from the Hund Corp. Based on measurements by Armbruster (1987). Two definitions of respirable dust are also included. (Adapted from Willeke and Baron, 1990.)

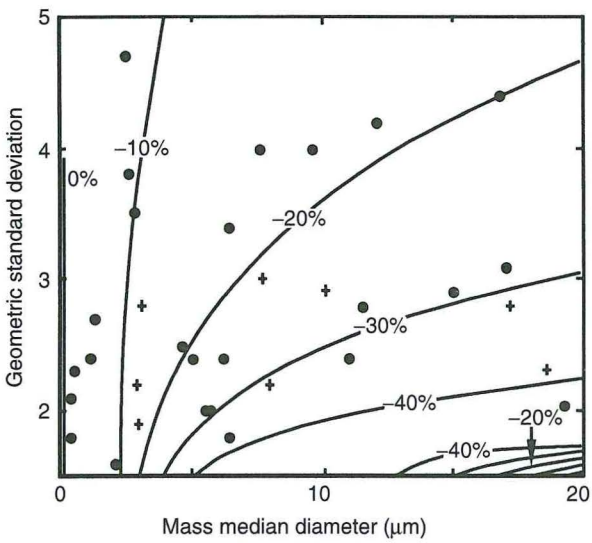

Fig. 7–11. Bias map comparing two defined respirable dust response curves for a range of lognormal size distributions. Data points represent distributions reported by (•) Hinds and Bellin (1988) and (+) Bowman et al. (1984).

tion ($d_{50} = 5\,\mu m$, $\sigma_g = 2.0$): non-light-absorbing DOP droplets and dense, light-absorbing iron oxide (Fe_2O_3) particles (Armbruster, 1987). The decline in response with increasing particle size above about 1 μm is common to all photometers. This decrease approximately corresponds to the classification characteristics of the ACGIH and BMRC definitions for respirable dust (ACGIH, 1999a,b), also indicated on Figure 7–9. Complex interactions between the incident light and the particle result in similarly complex response curve patterns that differ from one type of aerosol to another.

A photometer calibrated with one type of aerosol will, therefore, generally be biased if used to measure another aerosol with different chemistry or size distribution. This bias can be adjusted for a specific aerosol by drawing the aerosol through a filter downstream of or

parallel to the sensor and adjusting the sensor readout to equal the concentration measured using the filter. This procedure is valid as long as the type and size distribution of the aerosol remain unchanged. Instruments of this type can be used to make relative measurements, often providing useful real-time information, but should be used only with great care for situations requiring high accuracy.

One approach to evaluating the accuracy of a method over a wide range of aerosol size distributions is the use of a bias map (Caplan et al., 1977). This involves determining the range of size distributions over which the measurement is expected to occur. Hinds and Bellin (1988) reviewed aerosol distributions in more than 30 workplace operations and found size distributions with σ_g ranging from 1.5 to 5 and mass median aerodynamic diameters ranging from 0.1 to 20. One can examine the bias resulting from measurement of lognormal distributions throughout this range by comparison of one sampler versus a standard. As an example, calculation of the bias of the ACGIH definition versus the BMRC definition (Fig. 7–10) for each size distribution can be used to produce the bias map in Figure 7–11. This approach has been used to evaluate the optimum flow rate through a cyclone by comparing bias maps of the cyclone relative to a respirable dust definition at different flow rates (Bartley et al., 1994). Hinds and Bellin (1988) used their size-distribution data to estimate the effectiveness of respirators with measured size-dependent leakage.

REFERENCES

ACGIH. 1999a. *Particle Size-Selective Sampling of Particulate Air Contaminants*, ed. J. H. Vincent. Cincinnati, OH: American Conference of Governmental Industrial Hygienists.

ACGIH. 1999b. *Threshold Limit Values for Chemical Substances and Physical Agents*. Cincinnati, OH: American Conference of Governmental Industrial Hygienists.

Armbruster, L. 1987. A new generation of light-scattering instruments for respirable dust measurement. *Ann. Occup. Hyg.* 31:181–193.

Baron, P. A. 1984. Aerosol Photometers for respirable dust measurements. In *Manual of Analytical Methods*, 3rd Ed. (DHHS/NIOSH Pub. No. 84-100). Cincinnati, OH: National Institute for Occupational Safety and Health.

Baron, P. A. 1994. Asbestos and other fibers by PCM, Method 7400, Issue 2: 9/15/94. *NIOSH Manual of Analytical Methods, 3d eD.*, ed. P. M. Eller. (NIOSH) Pub. 84-100. Cincinnati, OH: National Institute for Occupational Safety and Health.

Baron, P. A. and G. J. Deye. 1990. Electrostatic effects in asbestos sampling I: Experimental measurements. *Am. Ind. Hyg. Assoc. J.* 51:51–62.

Baron, P. A. and K. Willeke. 1986. Respirable droplets from whirlpools: Measurements of size distribution and estimation of disease potential. *Environ. Res.* 39:8–18.

Bartley, D. L., C.-C. Chen, R. Song, and T. J. Fischback. 1994. Respirable aerosol sampler performance testing. *Am. Ind. Hyg. Assoc. J.* 55(11):1036–1046.

Blackford, D., A. E. Hansen, D. Y. H. Pui, P. Kinney, and G. P. Ananth. 1988. Details of recent work towards improving the performance of the TSI Aerodynamic Particle Sizer. In *Proceedings of the 2nd Annual Meeting of the Aerosol Society*. Bournemouth, U.K., March 22–24.

Bowman, J. D., D. L. Bartley, G. M. Breuer, L. J. Doemeny, D. J. Murdock. 1984. Accuracy criteria recommended for the certification of gravimetric coal mine dust samplers. Internal Report available from National Technical Information Service NTIS PB 85-222446. Cincinnati: National Institute for Occupational Safety and Health.

Buchan, R. M., S. C. Soderholm, and M. J. Tillery. 1986. Aerosol sampling efficiency of 37 mm filter cassettes. *Am. Ind. Hyg. Assoc. J.* 47:825–831.

Caplan, K. J., L. J. Doemeny, and S. D. Sorensen. 1977. Performance characteristics of the 10 mm cyclone respirable sampler: Part I—Monodisperse studies. *Am. Ind. Hyg. Assoc. J.* 38(2):83–95.

Currie, L. A. 1992. In pursuit of accuracy: Nomenclature, assumptions and standards. *Pure Appl. Chem.* 64:455–472.

Eisenhart, C., H. H. Ku, and R. Collé. 1990. Expression of the uncertainties of final measurement results: Reprints. In *Selected Publications for the EMAP Workshop.* NIST Internal Report 90-4272. Washington, DC: National Institute for Standards and Technology.

EPA. 1994. Guidance for the Data Quality Objectives Process, EPA QA/G4, in EPA/600/R-96/055. (Available at http://www.epa.gov/region10/www/offices/oea/qaindex.htm)

Gibson, J. D. 1971. *Nonparametric Statistical Inference.* New York: McGraw-Hill.

Hansen, A. G. 1985. Simulating the normal distribution. *BYTE* October:137–138.

Heitbrink, W. A., P. A. Baron, and K. Willeke. 1991. Coincidence in time-of-flight aerosol spectrometers: phantom particle creation. *Aerosol Sci. Technol.* 14:112–126.

Hinds, W. C. 1999. *Aerosol Technology.* New York: John Wiley & Sons.

Hinds, W. C. and P. Bellin. 1988. Effect of facial-seal leaks on protection provided by half-mask respirators. *Appl. Ind. Hyg.* 3:158–164.

Liu, B. Y. H., V. A. Marple, K. T. Whitby, and N. J. Barsic. 1974. Size distribution measurement of airborne coal dust by optical particle counters. *Am. Ind. Hyg. Assoc. J.* 8:443–451.

Liu, B. Y. H., D. Y. H. Pui, and W. Szymanski. 1985. Effects of electric charge on sampling and filtration of aerosols. *Ann. Occup. Hyg.* 29:251–269.

O'Brien, D. M., P. A. Baron, and K. Willeke. 1986. Size and concentration measurement of an industrial aerosol. *Am. Ind. Hyg. Assoc. J.* 47:386–392.

Okazaki, K., R. W. Wiener, and K. Willeke. 1987a. Isoaxial aerosol sampling: Non-dimensional representation of overall sampling efficiency. *Environ. Sci. Technol.* 21:178–182.

Okazaki, K., R. W. Wiener, and K. Willeke. 1987b. Non-isoaxial aerosol sampling: Mechanisms controlling the overall sampling efficiency. *Environ. Sci. Technol.* 21:183–187.

Pui, D. Y. H. 1996. Direct-reading instrumentation for workplace aerosol measurements—A review. *Analyst* 121:1215–1224.

Vincent, J. H. 1989. *Aerosol Sampling: Science and Practice.* New York: John Wiley & Sons.

Wake, D. 1989. Anomalous effects in filter penetration measurements using the aerodynamic particle sizer (APS 3300). *J. Aerosol Sci.* 20:1–7.

Willeke, K. and P. A. Baron. 1990. Sampling and interpretation errors in aerosol sampling. *Am. Ind. Hyg. Assoc. J.* 51:160–168.

Willeke, K. and B. Y. H. Liu. 1976. Single particle optical counter: Principles and application. In *Fine Particles: Aerosol Generation, Measurement, Sampling and Analysis*, ed. B. Y. H. Liu. New York: Academic Press.

Williams, K., C. Fairchild, and J. Jaklveic. 1993. Dynamic mass measurement techniques. In *Aerosol Measurement*, eds. K. Willeke and P. Baron. New York: Van Nostrand Reinhold.

AEROSOL MEASUREMENT

Principles, Techniques, and Applications

SECOND EDITION

Edited by

Paul A. Baron, Ph.D.
Physical Scientist
Centers for Disease Control and Prevention
National Institute for Occupational Safety and Health
Cincinnati, OH

Klaus Willeke, Ph.D.
Professor
Department of Environmental Health
University of Cincinnati
Cincinnati, OH

WILEY-INTERSCIENCE

A JOHN WILEY & SONS, INC., PUBLICATION

New York • Chichester • Weinheim • Brisbane • Singapore • Toronto

This book is printed on acid-free paper. ♾

Published simultaneously in Canada.

Library of Congress Cataloging-in-Publication Data:

Aerosol measurement : principles, techniques, and applications / [edited] by Paul A. Baron and Klaus Willeke.—2nd ed.

p. cm.

Includes index.

ISBN 0-471-35636-0 (cloth)

1. Aerosols—Measurement. 2. Air—Pollution—Measurement. I. Baron, Paul A., 1944– II. Willeke, Klaus.

TD884.5 .A33 2001

628.5'3'0287–dc21 2001017845

Printed in the United States of America.

10 9 8 7 6 5 4 3 2 1